Strong pattern selection and amplitude equation of higher order for ionization waves in a neon glow discharge

B. Bruhn and B.-P. Koch
Institut für Physik, Domstrasse 10a, 17487 Greifswald, Germany
(Received 29 June 1999)

Motivated by recent experiments and numerical simulations of the positive column of a neon glow discharge we investigate the Eckhaus instability of traveling waves. Compared to the classical results the plasma system shows some peculiarities, e.g., an asymmetric stability region and strong selection of periodic patterns. These complex phenomena may be explained by a transition from supercritical to subcritical Hopf bifurcation near the critical point. In the weak nonlinear region the wave dynamics is approximated by a quintic Ginzburg-Landau equation supplemented by nonlinear gradient terms. Starting from a hydrodynamic model the coefficients of this equation, which depend on the plasma parameters, are calculated. The stability properties of plane wave solutions are discussed for an infinitely long discharge as well as for finite ones. The theoretical results show most of the properties that are observed in real experiments.

PACS number(s): 52.35.Py, 52.80.Hc, 05.45.−a

I. INTRODUCTION

The study of nonlinear nonequilibrium phenomena in spatially extended systems is one of the very active areas in physics and other sciences. Pattern forming instabilities and pattern selecting processes attract the attention of both experimental and theoretical investigations [1]. An example for a physical system, which shows a very complex dynamical behavior, is the plasma of the positive column of inert gas discharges. One observes homogeneous states, periodic patterns, traveling waves, and different types of turbulent dynamics depending on pressure p_0, discharge current I_0, and geometry [2–4]. The topic considered here is the ionization instability in low-pressure neon discharges that arises above a critical value of the current. Mostly the theoretical description of ionization waves is investigated on the basis of a hydrodynamic model [5–7] in one spatial dimension. Starting from the homogeneous state of the positive column Hopf bifurcations are the generic wave forming processes and, moreover, different types of Hopf-Hopf bifurcations can be shown to exist [8]. Since such types of transitions occur in many different physical systems, it is desirable to find universal methods that allow one to extract some generic properties of the considered system.

The description of the wave dynamics near the instability border by means of amplitude equations is such a universal approach. For ionization waves close to the Pupp critical current, Bekki [9] has derived an amplitude equation that had the form of a nonlinear Schrödinger equation. Like this equation, also the Ginzburg-Landau equation is one of a few universal models describing the evolution of patterns in the weakly nonlinear region. There is enormous literature covering the field of the exact and approximate analytical solutions of the different Ginzburg-Landau models (cf. [10] and references therein). Moreover, the classification of the solution manifold by means of numerical methods is a well established instrument. For example, the borders separating regions of different behavior of the complex Ginzburg-Landau equation (CGLE) can be found in [11]. It is one important goal of the theoretical investigations of pattern formation to find the link between the basic evolution equations and the coefficients of the amplitude equation in question. These coefficients contain all relevant information of the underlying model in the weak nonlinear region.

In the field of ionization waves this is motivated by experimental investigations on the so-called *p* waves. Already in the experiments of Achterberg and Michel [13] some characteristics of the stability diagram were investigated. In recent experimental studies [14] the pecularities with respect to the modern theory of nonlinear systems are emphasized. The stability diagram indicates discharge currents of stable nonlinear wave states characterized by their wave number. Varying the current stable waves can be prepared. At the critical point the largest wave number appears. Increasing the current waves with smaller wave numbers occurs. Each one is characterized by its own stability range, which ends at a specific current. As a rule at a given current only one or two wave modes are permitted, i.e., with respect to the current there is overlapping of stability regions leading to hysteresis. The theoretical explanation may be attempted in the framework of the CGLE. In the limit of very long systems the stability borders that mark the so-called Eckhaus stability region in the plane of the wave number and the control parameter are given by a parabola centered at the critical wave number k_c. In a bounded system only discrete wave numbers exist. The main concern of this paper is to explain the experimentally found asymmetric stability region that strongly deviates from the expected behavior predicted by the CGLE.

There are additional facts making an extension of the usual Ginzburg-Landau description necessary. In a recent paper [12] we derived a modified CGLE near the border of ionization instability in a neon discharge using the multiple scale method. For different pressures the solutions of the CGLE were compared with numerical calculations of the full set of balance equations. For example, in the low-pressure region only traveling waves with one selected mode appear, whereas the CGLE predicts additionally intermittency in the corresponding parameter region (cf. [12]). Hence a CGLE

with third-order nonlinearity is not sufficient to describe the ionization waves at low-pressure values. The aim of this contribution is to show that higher-order terms of the modulated amplitude in the CGLE may explain these peculiarities observed in numerical simulations of the full set of balance equations and in real experiments. The amplitude equation in question is a quintic CGLE supplemented by nonlinear gradient terms, i.e.,

$$\frac{\partial A}{\partial t}=\mu A-v_g\frac{\partial A}{\partial z}+b\frac{\partial^2 A}{\partial z^2}+cA^*A^2+dA^{*2}A^3 +\left(a-i\frac{\partial c}{\partial k}\bigg|_0\right)A\frac{\partial A^*A}{\partial z}-i\frac{\partial c}{\partial k}\bigg|_0 A^*A\frac{\partial A}{\partial z}, \quad (1.1)$$

where $A(z,t)$ is the slowly varying amplitude and the coefficients (except for the group velocity v_g and the unfolding parameter μ) are complex numbers. It is the main technical task of this paper to derive the dependencies of these coefficients on plasma parameters. Compared to the standard CGLE of third order, the nonlinear gradient terms break the reflection symmetry $z\rightarrow -z$. This symmetry breaking provides an asymmetric stability region near the critical wave number [15] and influences the dynamical properties of localized solutions [16]. The term $v_g(\partial A/\partial z)$ breaks this symmetry, too, but it can be removed by transformation to a moving reference frame. To our knowledge, the investigated plasma system is the first one, where the strong selection of periodic patterns is observed in experiments and numerical simulations and is correctly described by a fifth-order amplitude equation.

Starting from a set of basic evolution equations in Sec. II, we derive (1.1) in Sec. III. Some results concerning plane waves and their stability are discussed in Sec. IV. Finally we discuss the validity of the results obtained.

II. BASIC EQUATIONS

The hydrodynamic description of ionization waves in the positive column plasma of a dc discharge is well accepted provided that the pressure is not to low. Starting from the set of balance equations for the density of electrons, ions, metastable atoms, and the electron temperature and using some physically motivated approximations [7], one finds a system of four nonlinear partial integrodifferential equations. The integrals arise from the coupling of the discharge through the external circuit, i.e., the voltage applied and the external resistance R_a [7,8]. In this paper we restrict our study to the limit of a very large external resistance ($R_a\rightarrow\infty$). Experimentally this can be realized by a discharge driven by a current source (cf. [14]). The limit $R_a\rightarrow\infty$ has the advantage that the basic equations reduce to partial differential equations, i.e., all integrals drop out and calculations are simplified. Although the external circuit is important for the understanding of the bifurcation behavior of ionization waves [7,8], its influence on the solution manifold of the amplitude equation is rather weak, at least in the considered region of plasma parameters [12]. In the limit $R_a\rightarrow\infty$ the set of basic equations can be written as

$$T_{jk}\frac{\partial X_k}{\partial t}=A_{jk}X_k+B_{jk}\frac{\partial X_k}{\partial z}+C_{jk}\frac{\partial^2 X_k}{\partial z^2}+D_{jkl}X_kX_l +Q_{jkl}X_k\frac{\partial X_l}{\partial z}+E_{jkl}X_k\frac{\partial^2 X_l}{\partial z^2}+F_{jkl}\frac{\partial X_k}{\partial z}\frac{\partial X_l}{\partial z} +G_{jklm}X_kX_lX_m+H_{jklm}X_kX_l\frac{\partial^2 X_m}{\partial z^2} +L_{jklm}X_k\frac{\partial X_l}{\partial z}\frac{\partial X_m}{\partial z}, \quad (2.1)$$

where $X_k=X_k(z,t)$ represents the four-dimensional wave vector and a summation is to be understood as one over repeated indexes ($j,k,l,\ldots=1,2,3,4$) unless the contrary is explicitly stated. The row vector components

$$(X_k)^T=(u,m,v,w)$$

are related to the radial averaged densities of charge carriers N, metastable atoms M, the electron temperature T, and the axial electric field E, i.e.,

$$u=\frac{N-N_0}{N_0},\quad m=\frac{M-M_0}{M_0},\quad v=\frac{T-T_0}{T_0},\quad w=\frac{E-E_0}{E_0}$$

denote the relative deviations from the homogeneous equilibrium state (N_0,M_0,T_0,E_0) [7]. The space and time variables z' and t' are transformed into a dimensionless form by

$$z=\frac{E_0}{T_0}z',\quad t=b_i\frac{E_0^2}{T_0}t',$$

where the electron temperature of the homogeneous state T_0 is measured in units of volts. b_i is the mobility of the ions.

The coefficients of the linear terms are given by

$$(T_{jk})=\begin{pmatrix}1&0&0&0\\0&1&0&0\\0&0&0&0\\0&0&0&0\end{pmatrix},$$

$$(A_{jk})=\begin{pmatrix}\eta_1&\eta_3&\eta_2&0\\\eta_4&\eta_6&\eta_5&0\\-1&-h_4&-h_1&1\\1&0&0&1\end{pmatrix},$$

$$(B_{jk})=\begin{pmatrix}0&0&0&0\\0&0&0&0\\0&0&\kappa&0\\\alpha&0&\beta&0\end{pmatrix},$$

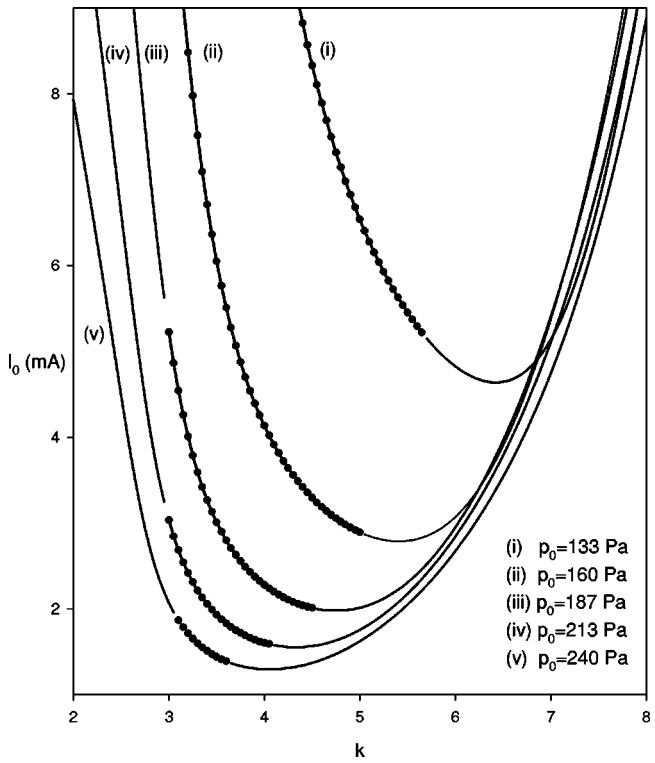

FIG. 1. Instability curves of p waves parametrized by selected pressure values. The homogeneous state becomes unstable above these curves. The transition to the unstable region is connected with a subcritical (black circles) or a supercritical (solid line) Hopf bifurcation. (Discharge radius $r_0=1$ cm and the dimensionless wave number k is normalized with respect to the equilibrium data T_0/E_0).

$$(C_{jk})=\begin{pmatrix} \alpha & 0 & \beta & 0 \\ 0 & D & 0 & 0 \\ -\delta_1 & 0 & -\delta_2 & 0 \\ 0 & 0 & 0 & 0 \end{pmatrix}. \tag{2.2}$$

The coefficients of the nonlinear terms $D_{jkl},\ldots,L_{jklm}$ can be found in the Appendix. Note that $\eta_1,\ldots,\eta_6$; $h_1,\ldots,h_6$; $\sigma_0,\ldots,\sigma_8$; and $\rho_1,\ldots,\rho_{10}$ are coefficients that result from a series expansion of the production and loss terms up to the third order (cf. [7,8]). In contrast to the kinetic coefficients $\alpha,\beta,\delta_1,\ldots,\delta_4$ and κ, which are assumed to be constant numbers, these parameters depend on the actual equilibrium solution, e.g., on the current I_0. The series expansion of the production and loss terms up to the third order is an approximation. Since collision rates are calculated by using empirical formulas (cf. [7]) terms of fourth and fifth order do not improve the precision of the results. Therefore (2.1) is our basic system and no further expansion terms of higher-order nonlinearity will be included.

In order to motivate the necessity of using Eq. (1.1), it is instructive to look for the bifurcation type (sub- or supercritical Hopf bifurcations) along the instability curve of the p waves. Figure 1 shows the results of such calculations for various values of the gas pressure p_0. These diagrams are obtained with the methods described in Ref. [8]. A transition between sub- and supercritical behavior can be observed near the minima of the instability curves. At these transition points, the real part of the coefficient of the nonlinear term in the Hopf normal form equation goes through zero. This type of degeneration is a necessary condition for the introduction of higher-order terms into a Ginzburg-Landau-type modulation equation [15,17].

The structure of Eq. (2.1) is sufficiently general in order to describe different physical systems, too. The coefficients $A_{jk},\ldots,L_{jklm}$ contain the particular properties of the system under consideration. Therefore, we shall derive the higher-order amplitude equation as general as possible and the link to the special plasma system will be made at the end of our considerations.

III. DERIVATION OF THE AMPLITUDE EQUATION

For clarity, a brief survey of the perturbation theoretical method is given (cf. [12,18]). Let ε be the small expansion parameter defined by

$$\varepsilon^2=\frac{I_0-I_c}{I_c}, \tag{3.1}$$

where the discharge current I_0 is the control parameter and I_c its value at the critical point. Then the wave vector X_k is expanded in a power series with respect to ε

$$X_k=\sum_{\alpha=1}^{\infty}\varepsilon^{\alpha}X_k^{(\alpha)}=\varepsilon X_k^{(1)}+\varepsilon^2X_k^{(2)}+\cdots \tag{3.2}$$

and each of these terms is represented by a Fourier series

$$X_k^{(\alpha)}=\sum_{N=-\infty}^{\infty}X_k^{(\alpha)N}(\tau,\xi)\exp iN(kz-\omega t). \tag{3.3}$$

The basic pair $(\omega,k)=(\omega_c,k_c)$ corresponds to the critical mode that becomes unstable at the minimum of the instability curve. The Fourier coefficients $X_k^{(\alpha)N}$ are weakly varying functions of space and time, i.e., they depend on stretched variables

$$\tau=\varepsilon^2t,\quad \xi=\varepsilon(z-vt), \tag{3.4}$$

where v is a free real parameter. Since the coefficients η_k, h_l, σ_m, ρ_n, and D depend on the discharge current I_0 (see [7] for their definitions), they also depend on ε. This dependence can be approximated by a Taylor expansion near the critical point (I_c,k_c), e.g.,

$$A_{jk}=A_{jk}|_0+\varepsilon^2A'_{jk}|_0+\frac{1}{2}\varepsilon^4A''_{jk}|_0+\cdots. \tag{3.5}$$

Here the prime stands for the partial derivative with respect to ε^2 and 0 indicates the critical point (I_c,k_c). The same expansion is used for the coefficients C_{jk}, D_{jkl}, and G_{jklm}. The remaining coefficients do not depend on ε since the kinetic coefficients α, β, δ_j, and κ are constant numbers.

Substituting all these expansions up to the fifth order with respect to the small parameter into the basic equations (2.1) and equating the coefficients of equal power of ε leads to a hierarchy of linear inhomogeneous problems. The corresponding equations can be solved by means of elementary

methods, however, the evaluations involve tedious algebra and therefore we report here only selected results.

A. First order of perturbation theory

Because of the property $X_k^{(\alpha)N}=(X_k^{(\alpha)-N})^*$ only the mode numbers $N\geqslant 0$ are relevant to our considerations. We define the mode-dependent linear operator Ω_{jk} by

$$\Omega_{jk}(N\omega,Nk)=-iN\omega T_{jk}-A_{jk}|_0-iNkB_{jk}+N^2k^2C_{jk}|_0. \tag{3.6}$$

Because the Fourier modes form an independent system of functions, the first order in ε yields an infinite system of homogeneous equations with a solution

$$X_k^{(1)0}=0,\quad X_k^{(1)N}=0 \text{ for } N\geqslant 2,$$

$$X_k^{(1)1}=\Phi_1(\xi,\tau)Y_k,\qquad (Y_k)=\begin{pmatrix}1\\ M_{10}\\ V_{10}\\ W_{10}\end{pmatrix}. \tag{3.7}$$

The components Y_k fulfill the homogeneous equations

$$\Omega_{jk}(\omega,k)Y_k=0 \tag{3.8}$$

and their explicit solution form can be found in [12] for our plasma system. The evaluation of the dispersion relation $\det(\Omega_{jk})=0$ yields the instability curves of the linear theory (cf. Fig. 1 and see also [12]). We note that $\Phi_1(\xi,\tau)$ is an arbitrary amplitude function that will be fixed at order ε^3. This is a typical property of the perturbation method used. At any order α a new amplitude $\Phi_\alpha(\xi,\tau)$ is introduced for the $N=1$ mode, which will be fixed by means of a partial differential equation at order $\alpha+2$.

Taking into account the usual Hermitian scalar product

$$\langle\vec{Y}|\vec{X}\rangle=Y_k^*X_k$$

the solution of the adjoint homogeneous problem can be found as

$$X_k^{ad}=\Psi(\xi,\tau)Y_k^{ad}, \tag{3.9}$$

where

$$\Omega_{jk}^{\dagger}Y_k^{ad}=0$$

and Ψ is an arbitrary amplitude. Furthermore, we choose $\Psi=1$ without any restriction. The explicit solution Y_k^{ad} can be found once more in [12].

B. Second order

To this order the mode numbers $N\geqslant 3$ provide the trivial solution. Hence, we consider the solutions for $N=2,1,0$ only. A more extended version of the second-order calculation is given in [12],

$$N=2:\quad X_k^{(2)2}=(\Phi_1)^2Y_k^{(2)2}, \tag{3.10}$$

where

$$\Omega_{jk}(2\omega,2k)Y_k^{(2)2}=\pi_j^{(2)2} \tag{3.11}$$

and the inhomogeneity can be calculated by

$$\pi_j^{(2)2}=[D_{jkl}|_0-k^2(E_{jkl}+F_{jkl})+ikQ_{jkl}]Y_kY_l.$$

The problem associated with the mode number $N=1$ can be solved explicitly,

$$N=1:\quad X_j^{(2)1}=\Phi_2Y_j-i\frac{\partial\Phi_1}{\partial\xi}\frac{\partial Y_j}{\partial k}, \tag{3.12}$$

where $\Phi_2=\Phi_2(\xi,\tau)$ is an unknown amplitude and, moreover, this order fixes the free parameter v in (3.4) to be the group velocity of the wave at the critical point

$$v=v_g=\left.\frac{\partial\omega}{\partial k}\right|_0. \tag{3.13}$$

The $N=0$ mode yields

$$N=0:\quad X_k^{(2)0}=\Phi_1^*\Phi_1Y_k^{(2)0} \tag{3.14}$$

with

$$\Omega_{jk}(0,0)Y_k^{(2)0}=\pi_j^{(2)0} \tag{3.15}$$

and

$$\pi_j^{(2)0}=ikQ_{jkl}(Y_k^*Y_l-Y_kY_l^*)+[D_{jkl}|_0+k^2(F_{jkl}-E_{jkl})]\times(Y_k^*Y_l+Y_kY_l^*). \tag{3.16}$$

The solution of (3.11) and (3.15) can be found by means of Kramer's rule or other standard methods.

C. Third order

Nontrivial solutions exist for $N=3,2,1,0$ and all other mode numbers $N\geqslant 0$ yield homogeneous systems that have the trivial solution only. For $N=3$ one finds

$$N=3:\quad X_k^{(3)3}=(\Phi_1)^3Y_k^{(3)3}, \tag{3.17}$$

where $Y_k^{(3)3}$ is independent on ξ,τ and fulfills the inhomogeneous equation

$$\Omega_{jk}(3\omega,3k)Y_k^{(3)3}=\pi_j^{(3)3} \tag{3.18}$$

with

$$\pi_j^{(3)3}=[D_{jkl}|_0-2k^2F_{jkl}](Y_kY_l^{(2)2}+Y_k^{(2)2}Y_l)+ikQ_{jkl}(2Y_kY_l^{(2)2}+Y_k^{(2)2}Y_l)-k^2E_{jkl}(4Y_kY_l^{(2)2}+Y_k^{(2)2}Y_l)+[G_{jklm}|_0-k^2(H_{jklm}+L_{jklm})]Y_kY_lY_m.$$

The inhomogeneous system corresponding to $N=2$ can directly be solved by means of the second-order solutions and one finds

$$N=2:\quad X_j^{(3)2}=2\Phi_1\Phi_2Y_j^{(2)2}-i\Phi_1\frac{\partial\Phi_1}{\partial\xi}\frac{\partial Y_j^{(2)2}}{\partial k}. \tag{3.19}$$

The mode $N=1$ requires a special consideration. The corresponding inhomogeneous problem has nontrivial solutions only if a Fredholm alternative condition is satisfied. This solvability condition leads to the CGLE (cf. also [12])

$$\frac{\partial\Phi_1}{\partial\tau}=p\Phi_1+b\frac{\partial^2\Phi_1}{\partial\xi^2}+c\Phi_1^*\Phi_1^2, \tag{3.20}$$

where the complex coefficients are given by

$$p=-i\frac{\partial\omega}{\partial\varepsilon^2}\bigg|_0,\quad b=\frac{i}{2}\frac{\partial^2\omega}{\partial k^2}\bigg|_0,\quad c=\frac{Y_j^{ad*}\pi_j^{(3)1}}{T_{lm}Y_l^{ad*}Y_m} \tag{3.21}$$

and the components $\pi_j^{(3)1}$ can be found in the Appendix. The explicit solution of the $N=1$ mode can be written as

$$X_j^{(3)1}=\Phi_3Y_j-i\frac{\partial\Phi_2}{\partial\xi}\frac{\partial Y_j}{\partial k}+\Phi_1\frac{\partial Y_j}{\partial\varepsilon^2}-\frac{1}{2}\frac{\partial^2\Phi_1}{\partial\xi^2}\frac{\partial^2Y_j}{\partial k^2}+\Phi_1^*\Phi_1^2Y_j^{(3)1}. \tag{3.22}$$

Here $\Phi_3=\Phi_3(\xi,\tau)$ is a new unknown amplitude and $Y_j^{(3)1}$ solves the equation

$$\Omega_{jk}(\omega,k)Y_k^{(3)1}=\pi_j^{(3)1}-cT_{jk}Y_k. \tag{3.23}$$

Of course, this inhomogeneous problem fulfills the solvability condition by taking into account the definition of c by (3.21). The solution $Y_k^{(3)1}$ strongly depends on the properties of the special matrix $\Omega_{jk}(\omega,k)$. In the case of our plasma system the rank of Ω_{jk} is three at least in the considered range of plasma parameters and therefore the solution can be found by $Y_4^{(3)1}=0$ and

$$\begin{pmatrix}\alpha k^2-\eta_1-i\omega & -\eta_3 & \beta k^2-\eta_2\\ -\eta_4 & Dk^2-\eta_6-i\omega & -\eta_5\\ 1-\delta_1k^2 & h_4 & h_1-i\kappa k-\delta_2k^2\end{pmatrix}\times\begin{pmatrix}Y_1^{(3)1}\\ Y_2^{(3)1}\\ Y_3^{(3)1}\end{pmatrix}=\begin{pmatrix}\pi_1^{(3)1}-cY_1\\ \pi_2^{(3)1}-cY_2\\ \pi_3^{(3)1}\end{pmatrix}. \tag{3.24}$$

This subsystem has an invertible coefficient matrix and can be solved by means of Kramer's rule.

The last step of the third perturbation order requires the study of the $N=0$ mode. The solution can be written as

$$N=0:$$

$$X_k^{(3)0}=(\Phi_1\Phi_2^*+\Phi_2\Phi_1^*)Y_k^{(2)0}+\Phi_1\frac{\partial\Phi_1^*}{\partial\xi}Y_k^{(3)0}+\Phi_1^*\frac{\partial\Phi_1}{\partial\xi}(Y_k^{(3)0})^*, \tag{3.25}$$

where the complex vector $Y_k^{(3)0}$ is a solution of

$$\Omega_{jk}(0,0)Y_k^{(3)0}=\pi_j^{(3)0} \tag{3.26}$$

with the inhomogeneity

$$\pi_j^{(3)0}=(v_gT_{jk}+B_{jk})Y_k^{(2)0}+i[D_{jkl}|_0+k^2(F_{jkl}-E_{jkl})]\times\left(Y_k\frac{\partial Y_l^*}{\partial k}+\frac{\partial Y_k^*}{\partial k}Y_l\right)+[Q_{jkl}+2ik(F_{jkl}-E_{jkl})]Y_kY_l^*+kQ_{jkl}\left(Y_k\frac{\partial Y_l^*}{\partial k}-\frac{\partial Y_k^*}{\partial k}Y_l\right). \tag{3.27}$$

Note that $\pi_j^{(3)0}$ is a complex valued inhomogeneity, whereas $X_k^{(3)0}$ represents a real valued solution. Without proof we give the following connection between the solutions of the second and third order for $N=0$:

$$-i\frac{\partial Y_k^{(2)0}}{\partial k}=(Y_k^{(3)0})^*-Y_k^{(3)0},$$

which can be used to check a numerical solution.

D. Fourth order

In this order it is sufficient to look at the mode numbers $N=0,1,2$ only because the higher-order nontrivial modes ($N=3,4$) do not contribute to the calculations of the nonlinear gradient terms and the term of fifth power in (1.1). Moreover, for $N=2$ and $N=0$ a particular (incomplete) solution is discussed, which simplifies all our calculations. We find

$$N=2:\quad X_k^{(4)2}=\Phi_1^*(\Phi_1)^3Y_k^{(4)2}+\cdots, \tag{3.28}$$

where the dots indicate further terms, e.g., terms that contain a derivative of Φ_1 with respect to ξ. But all these additional terms do not contribute to the fifth-order-term calculations. The vector $Y_k^{(4)2}$ in (3.28) is a solution of the inhomogeneous equation

$$\Omega_{jk}(2\omega,2k)Y_k^{(4)2}=-2cT_{jk}Y_k^{(2)2}+\pi_j^{(4)2}, \tag{3.29}$$

where the inhomogeneity results from all terms $\sim\Phi_1^*(\Phi_1)^3$ and c is defined by (3.21). The explicit form of $\pi_j^{(4)2}$ can be found in the Appendix. In a similar manner one obtains for the $N=0$ mode a particular solution

$$N=0:\quad X_k^{(4)0}=(\Phi_1^*\Phi_1)^2Y_k^{(4)0}+\cdots \tag{3.30}$$

and

$$\Omega_{jk}(0,0)Y_k^{(4)0}=-(c+c^*)T_{jk}Y_k^{(2)0}+\pi_j^{(4)0}. \tag{3.31}$$

This inhomogeneity $\pi_j^{(4)0}$ is given in the Appendix, too. We note that the first term of the right-hand side of (3.31) results from a term $-T_{jk}(\partial X_k^{(2)0}/\partial\tau)$. Inserting $X_k^{(2)0}$ given by Eq. (3.14) and using (3.20) by taking into account (3.30) provides the desired structure. Of course, (3.29) and (3.31) can be solved by means of a standard method.

In a next step we look for the solvability condition of the $N=1$ mode. After elementary manipulations one finds

$$\frac{\partial\Phi_2}{\partial\tau}=\cdots+a\Phi_1\frac{\partial(\Phi_1^*\Phi_1)}{\partial\xi}-i\frac{\partial c}{\partial k}\bigg|_0\frac{\partial(\Phi_1^*\Phi_1^2)}{\partial\xi}, \tag{3.32}$$

where the constant a is defined by

$$a=\frac{Y_j^{ad*}\left(\pi_j^{(4)1}+i\frac{\partial\pi_j^{(3)1}}{\partial k}\Big|_0\right)}{T_{lm}Y_l^{ad*}Y_m} \tag{3.33}$$

and the components of $\pi_j^{(4)1}$ are listed in the Appendix. The dots in (3.32) indicate further terms that are linear in Φ_2, for example, terms of the type $b(\partial^2\Phi_2/\partial\xi^2)$ or $c(\Phi_1^2\Phi_2^*+2\Phi_1^*\Phi_1\Phi_2)$. These additional terms correspond to the variational equation of (3.20) with $\delta\Phi_1\to\Phi_2$. Therefore the Fredholm solvability condition yields a linear inhomogeneous partial differential equation that fixes the second amplitude Φ_2. The inhomogeneity is formed by terms that contain the first amplitude Φ_1 and their derivatives [cf. (3.32)]. Beside the nonlinear gradient terms there are two additional linear terms of the type

$$\cdots+f\frac{\partial^3\Phi_1}{\partial\xi^3}+e\frac{\partial\Phi_1}{\partial\xi}$$

with coefficients

$$f=\frac{1}{6}\frac{\partial^3\omega}{\partial k^3}\Big|_0,\quad e=-\frac{\partial^2\omega}{\partial k\partial\varepsilon^2}\Big|_0. \tag{3.34}$$

However, as Eckhaus and Iooss [15] have shown, these linear terms can be shifted to higher-order corrections by means of a rescaling in the degenerated case (cf. also [17]). Therefore the nonlinear gradient terms are the only important contributions for our purpose.

E. Fifth order

In this order it is sufficient to examine the $N=1$ mode only. The solvability condition of the corresponding inhomogeneous problem yields a linear partial differential equation for the third amplitude $\Phi_3(\xi,\tau)$ that is introduced in the third order of perturbation theory [cf. (3.22)],

$$\frac{\partial\Phi_3}{\partial\tau}=\cdots+d\Phi_1^{*2}\Phi_1^3+\cdots, \tag{3.35}$$

where

$$d=\frac{Y_j^{ad*}[\pi_j^{(5)1}-(c^*+2c)T_{jk}Y_k^{(3)1}]}{T_{lm}Y_l^{ad*}Y_m}. \tag{3.36}$$

The dots in (3.35) indicate a lot of terms linear in Φ_3. Some of these terms depend on Φ_1 and Φ_2, however, we have written the most important inhomogeneous term only. The components of $\pi_j^{(5)1}$ can be found in the Appendix too. The calculation of the inhomogeneities $\pi_j^{(2)2},\ldots,\pi_j^{(5)1}$ is very intricate because the number of terms very strongly increases with the number of the perturbation order. Moreover, any of these terms (cf. $\pi_j^{(5)1}$ in the Appendix) contain some summations over the vector indexes that must be performed for the concrete physical system.

At this stage, the reconstruction of a general amplitude function $\Phi(\xi,\tau)$ is possible, which contains the contributions of successive orders [19]. Let

$$\Phi(\xi,\tau)=\Phi_1+\varepsilon\Phi_2+\varepsilon^2\Phi_3+\cdots$$

and taking into consideration the evolution Eqs. (3.20), (3.32), and (3.35) one finds

$$\frac{\partial\Phi}{\partial\tau}=p\Phi+b\frac{\partial^2\Phi}{\partial\xi^2}+c\Phi^*\Phi^2+\varepsilon\left[\left(a-i\frac{\partial c}{\partial k}\Big|_0\right)\Phi\frac{\partial\Phi^*\Phi}{\partial\xi}-i\frac{\partial c}{\partial k}\Big|_0\Phi^*\Phi\frac{\partial\Phi}{\partial\xi}+\cdots\right]+\varepsilon^2(d\Phi^{*2}\Phi^3+\cdots), \tag{3.37}$$

i.e., the usual CGLE with cubic order nonlinearity is a first approximation only of the wave dynamics of the full system near the instability border. The additional terms describe further details of the dynamics, for example, the $O(\varepsilon)$ terms break the reflection symmetry $\xi\to-\xi$ and the $O(\varepsilon^2)$ term models the influence of higher-order nonlinearities. From the mathematical point of view it is not quite clear whether such type of perturbation theory yields convergent results. We shall show in Sec. V that the additional terms produce some peculiarities we have observed in real experiments.

Finally, we return to the original space and time variables and introduce the amplitude function $\varepsilon\Phi(\xi,\tau)=\tilde{A}(z,t)$ to find

$$\frac{\partial\tilde{A}}{\partial t}=\varepsilon^2p\tilde{A}-v_g\frac{\partial\tilde{A}}{\partial z}+b\frac{\partial^2\tilde{A}}{\partial z^2}+c\tilde{A}^*\tilde{A}^2+d\tilde{A}^{*2}\tilde{A}^3+\left(a-i\frac{\partial c}{\partial k}\Big|_0\right)\tilde{A}\frac{\partial\tilde{A}^*\tilde{A}}{\partial z}-i\frac{\partial c}{\partial k}\Big|_0\tilde{A}^*\tilde{A}\frac{\partial\tilde{A}}{\partial z}.$$

A phase rotation

$$\tilde{A}(z,t)=\exp(i\varepsilon^2p_it)A(z,t),\qquad p=p_r+ip_i$$

removes the term $\sim p_i$ and we obtain

$$\frac{\partial A}{\partial t}=\varepsilon^2p_rA-v_g\frac{\partial A}{\partial z}+b\frac{\partial^2A}{\partial z^2}+cA^*A^2+dA^{*2}A^3+\left(a-i\frac{\partial c}{\partial k}\Big|_0\right)A\frac{\partial A^*A}{\partial z}-i\frac{\partial c}{\partial k}\Big|_0A^*A\frac{\partial A}{\partial z}, \tag{3.38}$$

which is the final form of the amplitude equation with the unfolding parameter

$$\mu=p_r\varepsilon^2=p_r\frac{I_0-I_c}{I_c}. \tag{3.39}$$

The coefficients can be calculated by means of (3.21), (3.33), and (3.36). Since the inhomogeneities $\pi_j^{(\alpha)N}$ depend on the solutions $Y_k^{(\beta)M}$ with $\beta<\alpha$, a successive evaluation of all inhomogeneous problems must be performed at the critical point.

IV. CONSTANT AMPLITUDE SOLUTIONS AND THEIR STABILITY

In this section plane wave solutions of the amplitude equation (3.38) of the form

$$A(z,t)=R\exp i[(k-k_c)]x+\Phi_0], \quad x=z-(v_g+u)t \tag{4.1}$$

are examined, where u, R, and Φ_0 are free real parameters. Splitting the complex parameters into real and imaginary parts

$$b=b_r+ib_i,\ \ c=c_r+ic_i,\ \ d=d_r+id_i,\ \ a=a_r+ia_i \tag{4.2}$$

and inserting (4.1) into (3.38) yields two real algebraic equations that determine R and u (cf. [20]). The wave amplitude can be written as

$$R^2=-\left[\frac{c_r+(k-k_c)\left.\frac{\partial c_r}{\partial k}\right|_0}{2d_r}-\sqrt{\Delta}\right]$$

with

$$\Delta=\frac{\left(c_r+(k-k_c)\left.\frac{\partial c_r}{\partial k}\right|_0\right)^2}{4d_r^2}-\frac{\varepsilon^2 p_r-b_r(k-k_c)^2}{d_r}. \tag{4.3}$$

This wave represents a real solution above of the instability border of the linear theory $\varepsilon^2 p_r=b_r(k-k_c)^2$. Additionally, there is an existence segment in the $(\varepsilon^2 p_r,k-k_c)$ plane bounded by the parabola $\Delta=0$ and the linear instability curve. We would like to note that these two parabolas are tangent at the point

$$(k-k_c)=-\frac{c_r}{\left.\frac{\partial c_r}{\partial k}\right|_0},\quad \varepsilon^2 p_r=\frac{b_r c_r^2}{\left(\left.\frac{\partial c_r}{\partial k}\right|_0\right)^2}. \tag{4.4}$$

There exists a second solution for R^2 with a positive sign in front of the root $\sqrt{\Delta}$ within this segment. But this second solution is unstable as Eckhaus and Iooss have shown [15]. Hence we investigate the stability properties of the first solution (4.3) only. There is a main result concerning its stability [15].

For sufficiently small values of $(k-k_c)$ and c_r, stable solutions of the type (4.3) can only exist in a small neighborhood of a single curve Γ in $(\mu,k-k_c)$ space. The curve Γ is a branch of a parabola that starts at the critical point.

This phenomenon is denoted as strong pattern selection, i.e., any value of the control parameter yields a unique wave number. In a neon glow discharge, we have observed experimentally a small stability band that is asymmetric with respect to the substitution $(k-k_c)\rightarrow-(k-k_c)$. The observed transitions show the peculiarities of an Eckhaus instability [14]. The same behavior is found in numerical simulations of the full set of balance equations [21].The width and the form of the stability band strongly depend on the plasma parameters, e.g., on the pressure p_0. In order to find these boundaries of the stability region close to Γ more precisely, we perform an analysis without the restriction to small values of $k-k_c$ and c_r. This analysis is made by means of the variational equation corresponding to (3.38)

$$\begin{aligned}\frac{\partial\delta A}{\partial t}=&\varepsilon^2 p_r\delta A+u\frac{\partial\delta A}{\partial x}+b\frac{\partial^2\delta A}{\partial x^2}+c(A^2\delta A^*+2A^*A\delta A)\\&+\left(a-i\left.\frac{\partial c}{\partial k}\right|_0\right)\left[A\frac{\partial}{\partial x}(A\delta A^*+A^*\delta A)\right.\\&\left.+\delta A\frac{\partial}{\partial x}(A^*A)\right]-i\left.\frac{\partial c}{\partial k}\right|_0\left[A^*A\frac{\partial}{\partial x}\delta A+(A\delta A^*\right.\\&\left.+A^*\delta A)\frac{\partial}{\partial x}A\right]+d(2A^3A^*\delta A^*+3A^{*2}A^2\delta A),\end{aligned}$$

where $\delta A(x,t)$ represents a small perturbation of the amplitude. Inserting the basic solution (4.1) for A and taking into consideration the complex conjugate variational equation yields a two-component vector differential equation. This equation can be simplified by means of a unitary transformation $\hat{U}$ of the type used in [12] and we find

$$\begin{aligned}\frac{\partial\vec{S}_1}{\partial t}=&\left(b_r\frac{\partial^2}{\partial x^2}+\left[u-2b_i(k-k_c)+R^2\left.\frac{\partial c_i}{\partial k}\right|_0\right]\frac{\partial}{\partial x}\right)\hat{I}\vec{S}_1\\&+\left(b_i\frac{\partial^2}{\partial x^2}+\left[2b_r(k-k_c)-R^2\left.\frac{\partial c_r}{\partial k}\right|_0\right]\frac{\partial}{\partial x}\right)\hat{K}\vec{S}_1\\&+2R^2\left(c_r+2R^2d_r+(k-k_c)\left.\frac{\partial c_r}{\partial k}\right|_0\right.\\&\left.+\left[a_r+\left.\frac{\partial c_i}{\partial k}\right|_0\right]\frac{\partial}{\partial x}\right)\hat{M}\vec{S}_1\\&+2R^2\left(c_i+2R^2d_i+(k-k_c)\left.\frac{\partial c_i}{\partial k}\right|_0\right.\\&\left.+\left[a_i-\left.\frac{\partial c_r}{\partial k}\right|_0\right]\frac{\partial}{\partial x}\right)\hat{P}\vec{S}_1,\end{aligned} \tag{4.5}$$

where the matrix operators are defined by

$$\hat{I}=\begin{pmatrix}1&0\\0&1\end{pmatrix},\ \ \hat{K}=\begin{pmatrix}0&-1\\1&0\end{pmatrix},\ \ \hat{M}=\begin{pmatrix}1&0\\0&0\end{pmatrix},\ \ \hat{P}=\begin{pmatrix}0&0\\1&0\end{pmatrix},$$

and

$$\begin{pmatrix}\delta A\\ \delta A^*\end{pmatrix}=\hat{U}\vec{S}_1.$$

The stability properties of $\vec{S}_1$ can be studied by means of the ansatz

$$\vec{S}_1(x,t)=[\vec{X}\cos(qx)+\vec{Y}\sin(qx)]\exp(\lambda t),$$

where $\vec{X},\vec{Y}$ are constant two-dimensional vectors and q is an arbitrary wave number. Inserting this ansatz into (4.5) we obtain a fourth-order algebraic equation that can be factorized resulting in

$$\lambda^2+(a_1+ib_1)\lambda+(a_0+ib_0)=0. \tag{4.6}$$

The real coefficients a_1,b_1,a_0,b_0 can be found in the Appendix. Note that (4.6) has the same form but different coefficients as in the case of Ref. [12]. Therefore we can use the corresponding stability conditions (cf. also [22])

$$a_1>0,\ \ P(q)=a_1^2a_0+(a_1b_1-b_0)b_0>0 \ \Leftrightarrow\ \text{stability}. \tag{4.7}$$

For a discussion of the long wavelength perturbations $q\to 0$, it is reasonable to introduce the rescaling transformation

$$\tilde{a}_0=\frac{a_0}{q^2},\ \ \tilde{b}_0=\frac{b_0}{q},\ \ \tilde{b}_1=\frac{b_1}{q},\ \ \tilde{a}_1=a_1\ \Rightarrow\ P(q)=q^2\tilde{P}(q). \tag{4.8}$$

Since $q^2\geqslant 0$ one also has the equivalent conditions

$$a_1>0,\ \ \tilde{P}(q)>0, \tag{4.9}$$

which are also applicable in the case $q\to 0$. Of course, (4.7) can be discussed numerically, if the discharge length l is finite and therefore a lower limit of the wave number of the perturbation exists. In an infinitely long system the stability against arbitrary long wavelength disturbances (i.e., $q\to 0$) can be studied by means of

$$\lim_{q\to 0}a_1=-2R^2\left(c_r+2R^2d_r+(k-k_c)\frac{\partial c_r}{\partial k}\bigg|_0\right)>0,$$

$$\lim_{q\to 0}\tilde{P}(q)>0. \tag{4.10}$$

After elementary substitutions the second condition (4.10) can be written as

$$\begin{aligned}
&-2R^2\left(b_r\left[c_r+2R^2d_r+(k-k_c)\frac{\partial c_r}{\partial k}\bigg|_0\right]+b_i\left[c_i+2R^2d_i+(k-k_c)\frac{\partial c_i}{\partial k}\bigg|_0\right]\right)\\
&-2R^2\left(2b_r(k-k_c)-R^2\frac{\partial c_r}{\partial k}\bigg|_0\right)\left[a_i-\frac{\partial c_r}{\partial k}\bigg|_0-\left(a_r+\frac{\partial c_i}{\partial k}\bigg|_0\right)\frac{c_i+2R^2d_i+(k-k_c)\frac{\partial c_i}{\partial k}\big|_0}{c_r+2R^2d_r+(k-k_c)\frac{\partial c_r}{\partial k}\big|_0}\right]\\
&-\left(2b_r(k-k_c)-R^2\frac{\partial c_r}{\partial k}\bigg|_0\right)^2\left(1+\frac{\left[c_i+2R^2d_i+(k-k_c)\frac{\partial c_i}{\partial k}\big|_0\right]^2}{\left[c_r+2R^2d_r+(k-k_c)\frac{\partial c_r}{\partial k}\big|_0\right]^2}\right)>0,
\end{aligned} \tag{4.11}$$

where R^2 is defined by (4.3). Equation (4.11) can be considered as a function $f(k-k_c,\mu)>0$ since R^2 depends on $\mu=\varepsilon^2p_r$ and $(k-k_c)$. There are two marginal cases, where (4.11) reduces to well known results. Without proof we note that in the limit $d_r,d_i,a_r,a_i,\partial c_r/\partial k|_0,\partial c_i/\partial k|_0\to 0$ the stable band of the usual CGLE arises (see, e.g., [23]). The second case yields the stability curve Γ found by Eckhaus and Iooss [15]. Let the magnitude of c_r and $k-k_c$ be sufficiently small by

$$c_r=\varepsilon\tilde{c}_r,\ \ k-k_c=\varepsilon\tilde{k}. \tag{4.12}$$

Then by taking into account (4.3), the amplitude of the wave is small, too,

$$R^2=\varepsilon\tilde{R}^2,$$

where the tilde quantities are $O(1)$. Inserting the assumptions (4.12) into (4.11) and considering the resulting expression as a power series with respect to the small parameter ε, one finds

$$\begin{aligned}
0<&-\frac{c_i^2\left(2b_r\tilde{k}-\tilde{R}^2\frac{\partial c_r}{\partial k}\big|_0\right)^2}{\left(\tilde{c}_r+2\tilde{R}^2d_r+\tilde{k}\frac{\partial c_r}{\partial k}\big|_0\right)^2}\\
&+\varepsilon\left[-2b_ic_i\tilde{R}^2+\left(2b_r\tilde{k}-\tilde{R}^2\frac{\partial c_r}{\partial k}\bigg|_0\right)(\cdots)\right]+O(\varepsilon^2).
\end{aligned} \tag{4.13}$$

The dots indicate some terms that are not important in our discussion. The first term on the right-hand side is negative

TABLE I. Dependence of the coefficients of the amplitude equation on the pressure p_0.

p_0 (Pa)	v_g	b_r	b_i	c_r	c_i	$\left.\frac{\partial c_r}{\partial k}\right\|_0$	$\left.\frac{\partial c_i}{\partial k}\right\|_0$	a_r	a_i	d_r	d_i
160	−0.192	0.0917	−0.0156	−2.220	10.1	−6.63	4.90	−8.50	3.39	−329.2	−2203.2
187	−0.139	0.0740	−0.0142	−0.776	5.11	−3.59	2.53	−4.64	−0.363	−111.1	−744.4
200	−0.127	0.070	−0.0112	−0.593	4.09	−2.84	1.88	−3.70	−0.678	−70.6	−491.0
213	−0.120	0.0676	−0.0079	−0.529	3.43	−2.32	1.47	−3.11	−0.759	−47.1	−344.8
240	−0.115	0.0653	−0.0018	−0.526	2.64	−1.70	1.04	−2.47	−0.750	−23.9	−195.4
267	−0.115	0.0646	0.0036	−0.559	2.21	−1.38	0.849	−2.17	−0.724	−14.1	−126.1
293	−0.119	0.0650	0.0084	−0.595	1.96	−1.20	0.758	−2.02	−0.716	−9.54	−89.1
320	−0.123	0.0656	0.0128	−0.628	1.81	−1.09	0.714	−1.95	−0.724	−7.22	−67.2
347	−0.129	0.0666	0.0170	−0.662	1.73	−1.04	0.697	−1.93	−0.743	−5.96	−53.4
373	−0.136	0.0680	0.0211	−0.699	1.69	−1.01	0.694	−1.94	−0.770	−5.23	−44.1
400	−0.144	0.0696	0.0252	−0.739	1.68	−1.00	0.702	−1.98	−0.803	−4.79	−37.6
427	−0.152	0.0713	0.0294	−0.783	1.70	−1.01	0.717	−2.04	−0.841	−4.52	−32.9
453	−0.161	0.0731	0.0338	−0.833	1.73	−1.02	0.738	−2.12	−0.884	−4.34	−29.5
480	−0.171	0.0751	0.0383	−0.889	1.78	−1.04	0.764	−2.21	−0.931	−4.21	−27.0
507	−0.181	0.0772	0.0431	−0.951	1.85	−1.07	0.794	−2.32	−0.984	−4.11	−25.1
533	−0.192	0.0793	0.0481	−1.02	1.93	−1.11	0.827	−2.44	−1.04	−4.00	−23.7
560	−0.204	0.0815	0.0534	−1.10	2.02	−1.14	0.864	−2.58	−1.10	−3.89	−22.7
587	−0.216	0.0839	0.0591	−1.18	2.13	−1.19	0.905	−2.73	−1.17	−3.75	−22.0
1200	−0.723	0.323	−0.352	−1.56	1.62	−2.68	−0.225	2.20	−1.59	−9.11	1.67

and therefore the stability condition can only be fulfilled for all sufficiently small values of $\varepsilon>0$ if this term vanishes, i.e.,

$$\left(2b_r\tilde{k}-\tilde{R}^2\left.\frac{\partial c_r}{\partial k}\right|_0\right)=0. \tag{4.14}$$

Here we have assumed $c_i\neq 0$. Moreover, (4.13) reduces to

$$0<\varepsilon[-2b_ic_i\tilde{R}^2]+O(\varepsilon^2)$$

i.e., an additional condition arises by

$$b_ic_i<0. \tag{4.15}$$

Rescaling (4.14) according to (4.12) one finds

$$2b_r(k-k_c)-R^2\left.\frac{\partial c_r}{\partial k}\right|_0=0. \tag{4.16}$$

This equation defines the stability curve Γ. Using similar abbreviations as Eckhaus and Iooss [15]

$$k_0=c_r\left(\left.\frac{\partial c_r}{\partial k}\right|_0\right)^{-1},$$

$$s=\left(\frac{1}{2}\left.\frac{\partial c_r}{\partial k}\right|_0\right)^2+d_rb_r, k_*=-\frac{k_0}{4s}\left(\left.\frac{\partial c_r}{\partial k}\right|_0\right)^2,$$

$$\varepsilon_*^2=\frac{b_rk_0^2}{4p_rs}\left(\left.\frac{\partial c_r}{\partial k}\right|_0\right)^2, \tag{4.17}$$

we find after simple calculations

$$\Gamma:\ 4b_rs[(k-k_c)-k_*]^2+p_r\left(\left.\frac{\partial c_r}{\partial k}\right|_0\right)^2(\varepsilon^2-\varepsilon_*^2)=0. \tag{4.18}$$

A detailed discussion of the properties of this curve can be found in [15].

Since we are interested in the boundaries of the stability band around Γ, a numerical evaluation of (4.11) is possible in all cases in which the restriction (4.12) fails. We report on selected results concerning the ionization waves in the next section.

V. DISCUSSION OF THE STABILITY PROPERTIES OF IONIZATION WAVES

In order to predict the stability properties of ionization waves in a neon glow discharge we have to solve two problems. In a first step one has to calculate the complex coefficients of the amplitude equation (3.38). These coefficients contain all information on the special plasma system that is relevant to the wave dynamics in the weak nonlinear region. The dependence of these coefficients on the plasma parameters, e.g., p_0 or r_0, is not easy to discuss because some intermediate steps, such as the solution of inhomogeneous systems, must be performed (cf. Sec. III). Therefore, these coefficients were determined numerically by solving the inhomogeneous problems discussed in Sec. III for selected pressure values and a fixed radius $r_0=1$ cm. The results are shown in Table I. We observe a strong variation of some of the coefficients (e.g., a_r, d_r, and d_i) as the pressure increases. These coefficients are large in the low-pressure region $p_0<250$ Pa. Taking into consideration the amplitude equation (3.37) found by means of perturbation theory, we expect that the additional nonlinearities are very important in

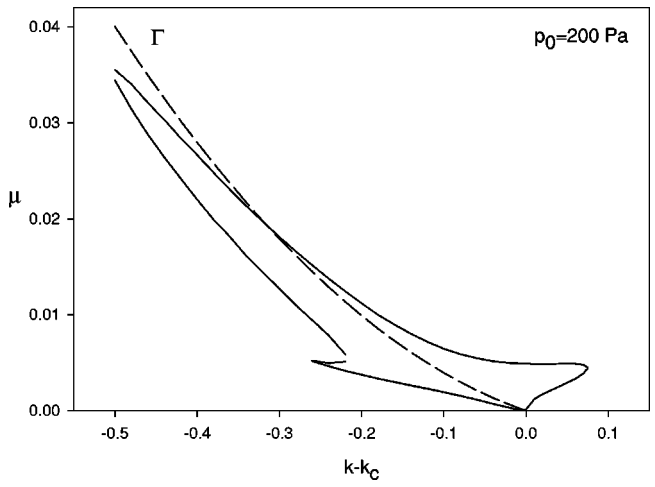

FIG. 2. Stability band of an infinitely long discharge ($p_0=200$ Pa, $r_0=1$ cm) calculated from condition (4.11) and Table I. The solid lines indicate the boundaries of the stability region, i.e., outside of the band the p waves become unstable. The dashed line marks the theoretical stability curve Γ defined by (4.18). k is the dimensionless wave number and the corresponding critical values are given by $k_c=4.512$, $I_c=1.736$ mA, where $p_r=0.254$.

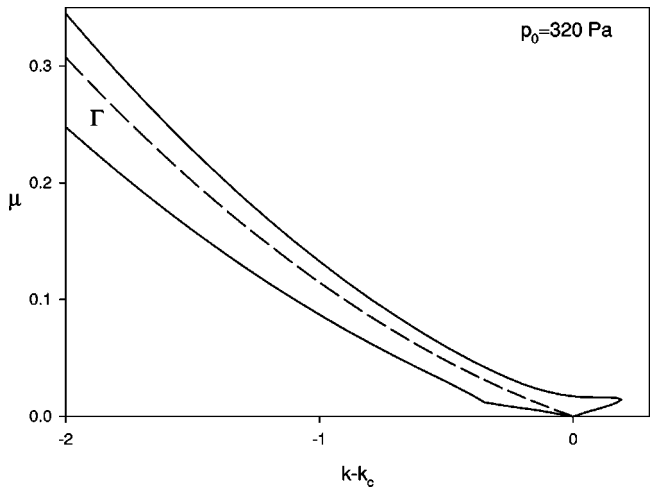

FIG. 3. Stability band of an infinitely long discharge ($p_0=320$ Pa, $r_0=1$ cm) calculated from condition (4.11) and Table I. The solid lines indicate the boundaries of the stability region, i.e., outside of the band the p waves become unstable. The dashed line marks the theoretical stability curve Γ defined by (4.18). k is the dimensionless wave number and the corresponding critical values are given by $k_c=3.640$, $I_c=0.915$ mA, where $p_r=0.191$.

this pressure range. On the other hand, we find that c_r is small compared to other coefficients (cf. a_r, d_r, d_i), but it is not ''very'' small over the whole pressure region. The essential condition that has to be fulfilled by the coefficients requires that the ratio c_r/d_r is a sufficiently small quantity [17]. For example, the following modified scaling transformation

$$b_r=\varepsilon\tilde{b}_r,\quad b_i=\varepsilon\tilde{b}_i,\quad d_r=\varepsilon^{-1}\tilde{d}_r,\quad d_i=\varepsilon^{-1}\tilde{d}_i,\quad c_r=\varepsilon\tilde{c}_r,$$

$$k-k_c=\varepsilon\tilde{k},\quad p_r=\varepsilon\tilde{p}_r, \tag{5.1}$$

where the wave amplitude scales as $R^2=\varepsilon^2\tilde{R}^2$, can be used instead of (4.12) here. Inserting (5.1) into (4.11) and performing a similar treatment as in Sec. IV provides exactly the same results, i.e., the curve Γ according to (4.14) and the stability condition (4.15). Therefore we expect also the strong pattern selection property in the case of our particular coefficients. The second step of our consideration contains the numerical evaluation of the condition (4.11). Figure 2 shows the stability region for a pressure $p_0=200$ Pa. Remember that the unfolding parameter μ is proportional to the current deviations from the critical value [see Eq. (3.39)].

In contrast to the classical Eckhaus result we find a stability band of finite length that is asymmetric with respect to the transformation $(k-k_c)\rightarrow-(k-k_c)$ and is bent to smaller wave numbers. This behavior is observed in a real neon discharge and the corresponding transitions between the stable and unstable regions, respectively, are identified as an Eckhaus-type instability [14]. We would like to note that a similar stability band has been observed already by Achterberg and Michel [13] in experiments, however, they could not realize the essential nonlinear nature of this phenomenon.

For all sufficiently small values of μ and $k-k_c$ the curve Γ lies within the stability band, but for $k-k_c<-0.3$ we observe an increasing deviation. This is not surprising since the stability curve Γ is an approximation. An interesting property of the stability region for this pressure value is the existence of a lower bound with respect to the wave number, i.e., no stable waves exist for $k-k_c<-0.5$. In contrast, the stability region of the full system of balance equations does not have this property [21]. The reason for this difference seems to be that the amplitude equation is an approximation of the full system near the critical point. The lower bound with respect to the wave number strongly increases with pressure. Figure 3 shows the results in the case of $p_0=320$ Pa. We did not find a lower limit of the wave number for all $k-k_c>-3.0$ and, moreover, the curve Γ lies perfectly within the band. But there is still a contradiction to the theoretical results discussed in Sec. IV: Inspecting the corresponding coefficients of Table I we find $b_ic_i>0$, i.e., there must be unstable waves only [cf. (4.15)]. This example shows clearly the limits of the analytical estimations of Sec. IV, especially the restricted applicability of (4.15). The stability function (4.11) is positive, but very small. Therefore it is hard to attack by means of the mentioned type of perturbation theory. Our results in the case $b_ic_i>0$ are confirmed by numerical simulations of the full set of hydrodynamic balance equations at selected pressure values, which yield the same stability properties [21]. Moreover, also the real experiment shows stable waves in the same pressure region [13,24].

Increasing the pressure p_0, one finds a enlargement of the stability region, which finally yields a loss of the strong pattern selection property. Such a situation is presented in Fig. 4 for $p_0=1200$ Pa. Note that one observes the so-called s waves [25] at this pressure value near the instability boundary. Although the curve Γ exists in this case ($b_ic_i<0$), it has no practical meaning because the stability region fills a large portion of the $(\mu,k-k_c)$ plane. The stability region is similar to that of the cubic order CGLE, which shows that the higher-order nonlinear terms are not very important for these plasma parameters. Moreover, the applicability of the degenerate modulation equation is doubtful in this case. A correct

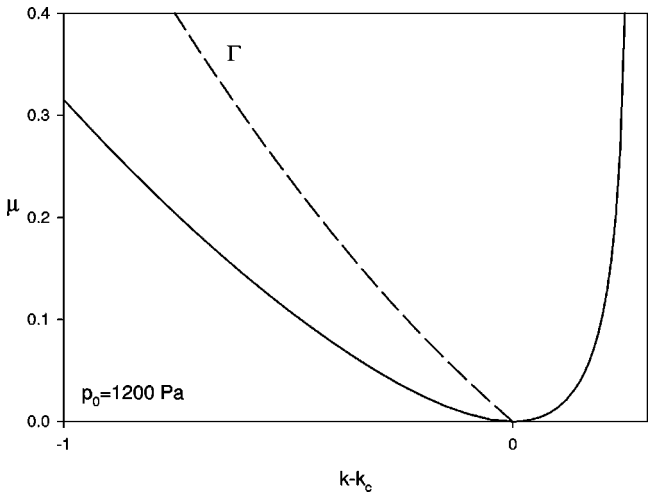

FIG. 4. Stability region (above the solid line) of s waves in an infinitely long discharge ($p_0=1200$ Pa, $r_0=1$ cm) calculated from condition (4.11) and Table I. The dashed line marks the theoretical stability curve Γ defined by (4.18). The corresponding critical values are given by $k_c=1.092$, $I_c=1.039$ mA, and $p_r=0.368$.

description must include the two additional linear terms of the fourth perturbation order. We have estimated the coefficient f according to (3.34) and found the ratio $|f|/|b|\approx 0.3$. This means that the results of Fig. 4 are correct at least for sufficiently small values of $(k-k_c)$. In order to study the influence of a finite length on the stability properties of p waves, we have performed some additional considerations. In a finite column only a discrete set of wave numbers $k=k_n=2\pi n/l$ $(n=1,2,\ldots)$ can be realized. This means that due to the strong pattern selection one finds a subset of k_n with finite intervals of control parameter values where the waves are stable. Of course, the width of the intervals is affected by the actual plasma parameters. Whether or not the neighboring intervals overlap strongly depends on the width of the stability band and on the realized wave numbers of the system. Moreover, if the discharge has a finite length l, a lower limit of the wave number q of the perturbation exists, which is given by

$$q_{min}=2\pi/l. \tag{5.2}$$

In this case the stability conditions (4.10) and (4.11) are not applicable since they are based on the limit $q\rightarrow 0$. Of course, we can use the general condition (4.7), where the substitution $q\rightarrow q_{min}$ must be made. Then the polynomial $P(q_{min})$ depends on the length l and can be studied by means of numerical methods. The results of two different lengths are represented in Figs. 5 and 6 for a pressure $p_0=200$ Pa. Here we have marked the set of realized stable wave numbers $k_n=2\pi n/l$ by vertical lines. Note that the length of the discharge L is connected to the dimensionless length l by a factor E_0/T_0 [7], where E_0 and T_0 are the equilibrium values of the electric field and the electron temperature, respectively. The principal shape of the band remains unchanged as the length l is varied (cf. also Fig. 2), but one observes a minor enlargement of the stability region as the length of the discharge decreases. We expect that this relatively small effect cannot be observed in a real neon discharge. On the other hand, the finite length of the stability band at p_0

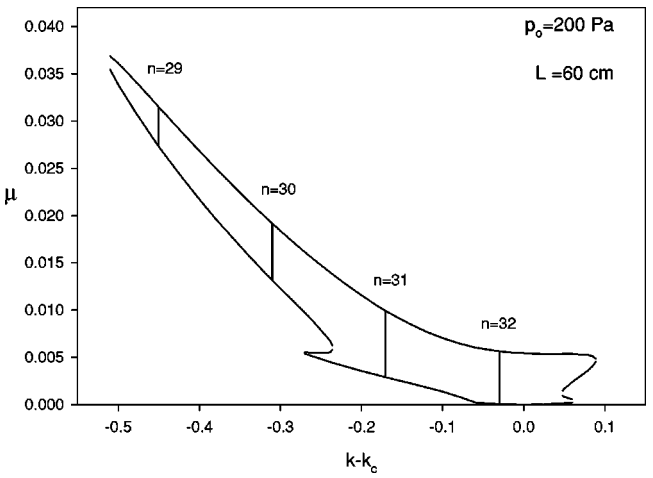

FIG. 5. Stability band (solid lines) and sets of stable wave numbers (vertical lines with corresponding mode numbers) of p waves in a system with length $L=60$ cm ($p_0=200$ Pa, $r_0=1$ cm) calculated from condition (4.7) and Table I. The critical values are the same as in Fig. 2.

$=200$ Pa restricts the number of observable stable p wave modes. For example, there are only two stable modes in a discharge of length $L=30$ cm at $p_0=200$ Pa. This number of stable modes increases as the pressure increases for a fixed discharge length. Figure 7 shows the corresponding stability band in the case of $p_0=320$ Pa. This seems to be the typical situation as observed in real experiments [13,14]. Starting with a stable wave mode the Eckhaus instability appears by increasing or decreasing the current I_0, so that the stability band is left and a transition to the neighboring stable wave mode occurs. Since there are overlapping stability intervals, a hysteresis is observed if the current is varied. This effect cannot be described by means of the usual cubic order CGLE because the resulting stability region is bounded by a parabola that cannot be left by increasing the control parameter (the current I_0). As a consequence the observed hysteresis [14] is an important argument for the necessity of using an amplitude equation of higher order as (3.38).

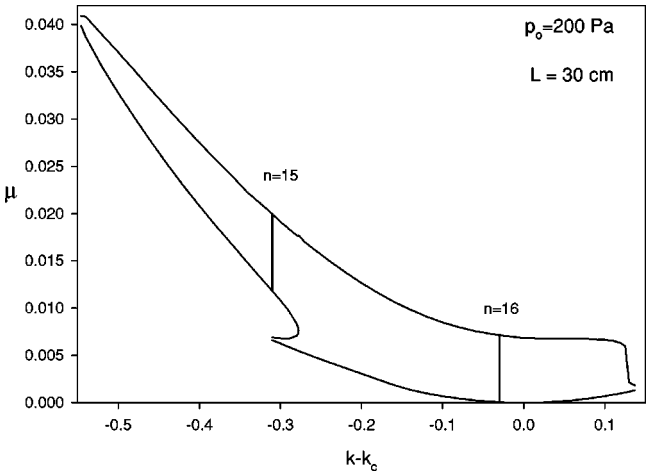

FIG. 6. Stability band (solid lines) and sets of stable wave numbers (vertical lines with corresponding mode numbers) of p waves in a system with length $L=30$ cm ($p_0=200$ Pa, $r_0=1$ cm) calculated from condition (4.7) and Table I. The critical values are the same as in Fig. 2.

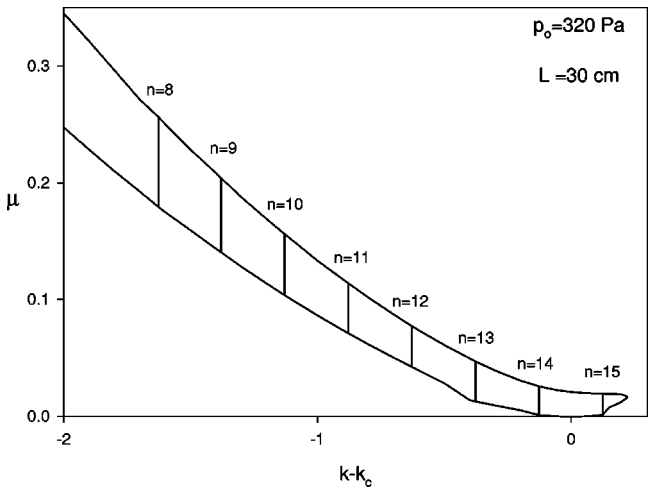

FIG. 7. Stability band (solid lines) and sets of stable wave numbers (vertical lines with corresponding mode numbers) of p waves in a system with length $L=30$ cm ($p_0=320$ Pa, $r_0=1$ cm) calculated from condition (4.7) and Table I. The critical values are the same as in Fig. 3.

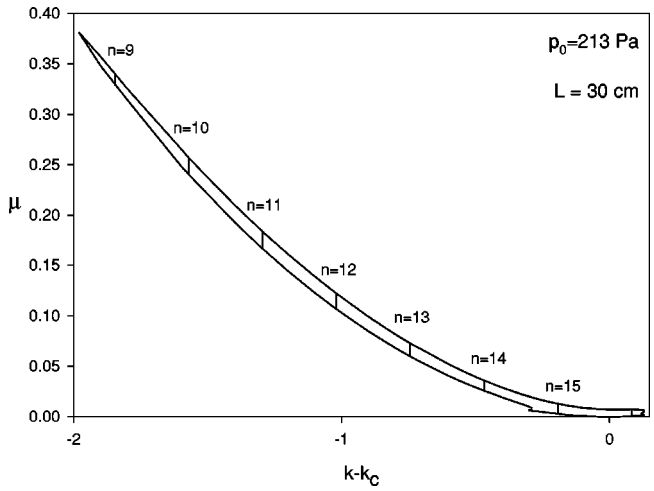

FIG. 8. Stability band (solid lines) and sets of stable wave numbers (vertical lines with corresponding mode numbers) of p waves in a system with length $L=30$ cm ($p_0=213$ Pa, $r_0=1$ cm) calculated from condition (4.7) and Table I. The corresponding critical values are given by $k_c=4.326$, $I_c=1.553$ mA, where $p_r=0.234$.

Our last example given in Fig. 8 shows the possibility of finding nonoverlapping stability intervals of the control parameter (e.g., modes $n=12$ and $n=13$). On the contrary at $p_0=320$ Pa and $L=30$ cm (cf. Fig. 7) one finds one overlap only. The nonoverlapping is accompanied by unstable wave dynamics if the discharge current I_0 is choosen in the gap between the two neighboring stability ranges. In such cases one observes irregular transitions between two wave modes in the numerical simulation of the full set of balance equations. A numerical study concerning the pattern selecting instabilities can be found in [21].

In our opinion, not all of these details concerning the stability properties can be found also in real experiments at the same values of the plasma parameters. However, the qualitative description of the wave phenomena by means of amplitude equations seems to be a good instrument to understand most of the nonlinear properties near the bifurcation point. The results of this paper give rise to additional questions on the details of the transition from the stability band to the instability region (cf. Figs. 2–8). In numerical simulations [21] two types of the Eckhaus instability have been detected. If one leaves the stability band by reducing the discharge current always the subcritical Eckhaus instability is observed, where the long wavelength perturbation increases in time until a space-time dislocation evolves. On the upper border of the stability band at certain parameter sets a supercritical bifurcation may appear. In this case one observes a stable long wavelength perturbation, whose amplitude increases proportional to the square root of the current increase. Hitherto such bifurcations have been found in Rayleigh-Bénard convection [26] and in hydrothermal waves [27]. The theoretical analysis can be accomplished starting from Eq. (1.1) and using the coefficients of Table I. Further phenomena, which we plan to investigate, are spatiotemporal intermittency and the propagation of localized solutions [16].

ACKNOWLEDGMENTS

We acknowledge useful discussions with P. Jonas, A. Dinklage, C. Wilke, and H. Deutsch. This work was supported by the Deutsche Forschungsgemeinschaft through ''Sonderforschungsbereich 198: Kinetik partiell ionisierter Plasmen.''

APPENDIX A: DEFINITIONS

In this Appendix we list some of our abbreviations and definitions. We begin with the definition of the nonlinear coefficients of the basic equation (2.1), where only the nonzero coefficients are given

$$D_{jkl}:$$

$$D_{113}=D_{131}=\rho_1/2,\ \ D_{122}=\rho_5,\ \ D_{133}=\rho_2,\ \ D_{112}=D_{121}=\rho_3/2,$$

$$D_{123}=D_{132}=\rho_4/2,\ \ D_{213}=D_{231}=\rho_6/2,\ \ D_{233}=\rho_7,\ \ D_{222}=\rho_{10},$$

$$D_{212}=D_{221}=\rho_8/2,\ \ D_{223}=D_{232}=\rho_9/2,\ \ D_{313}=D_{331}=-h_1/2,$$

$$D_{312}=D_{321}=-h_4/2,\ \ D_{323}=D_{332}=-h_5/2,\ \ D_{414}=D_{441}=1/2,$$

$$D_{333}=-h_2,$$

$$E_{jkl}:$$

$$E_{131}=\alpha,\ \ E_{113}=\beta,\ \ E_{331}=-2\delta_1,\ \ E_{313}=-\delta_2,\ \ E_{333}=-\delta_2,$$

$$F_{jkl}:$$

$$F_{113}=F_{131}=(\alpha+\beta)/2,\ \ F_{313}=F_{331}=-\delta_3/2,\ \ F_{333}=-\delta_2,$$

$$Q_{jkl}:$$

$$Q_{413}=\beta,\ \ Q_{431}=\alpha.$$

The cubic order coefficients are given by

$$G_{jklm}:$$

$$G_{1123}=G_{1231}=G_{1312}=G_{1132}=G_{1321}=G_{1213}=\sigma_0/6,\ \ G_{1333}=\sigma_2,$$

$$G_{1133}=G_{1331}=G_{1313}=\sigma_1/3,\ \ G_{1233}=G_{1332}=G_{1323}=\sigma_3/3,$$

$$G_{1223}=G_{1232}=G_{1322}=\sigma_4/3,\ \ G_{2133}=G_{2331}=G_{2313}=\sigma_5/3,$$

$$G_{2233}=G_{2332}=G_{2323}=\sigma_7/3,\ \ G_{2223}=G_{2232}=G_{2322}=\sigma_8/3,$$

$$G_{3133}=G_{3331}=G_{3313}=-h_2/3,\ \ G_{2333}=\sigma_6,\ \ G_{3333}=-h_3,$$

$$G_{3123}=G_{3231}=G_{3312}=G_{3132}=G_{3321}=G_{3213}=-h_5/6,$$

$$G_{3233}=G_{3332}=G_{3323}=-h_6/3,$$

$$H_{jklm}:$$

$$H_{3331}=-\delta_1,\ \ H_{3133}=H_{3313}=-\delta_2/2,$$

$$L_{jklm}:$$

$$L_{3133}=-\delta_2,\ \ L_{3313}=L_{3331}=-\delta_3/2.$$

Next we list the inhomogeneities used in Sec. III. Note that all vector components and the wave number must be evaluated at the critical pair (k_c,ω_c)

$$\begin{aligned}\pi_j^{(3)1}=&2k^2F_{jkl}(Y_k^*Y_l^{(2)2}+Y_k^{(2)2}Y_l^*)-k^2E_{jkl}(4Y_k^*Y_l^{(2)2}+Y_k^{(2)2}Y_l^*+Y_k^{(2)0}Y_l)+ikQ_{jkl}(2Y_k^*Y_l^{(2)2}-Y_k^{(2)2}Y_l^*+Y_k^{(2)0}Y_l)\\&+D_{jkl}|_0(Y_k^*Y_l^{(2)2}+Y_k^{(2)2}Y_l^*+Y_kY_l^{(2)0}+Y_k^{(2)0}Y_l)+[G_{jklm}|_0-k^2H_{jklm}](Y_kY_lY_m^*+Y_k^*Y_lY_m+Y_kY_l^*Y_m)\\&+k^2L_{jklm}(Y_kY_lY_m^*-Y_k^*Y_lY_m+Y_kY_l^*Y_m),\end{aligned}$$

$$\begin{aligned}\pi_j^{(4)2}=&D_{jkl}|_0(Y_k^{(2)2}Y_l^{(2)0}+Y_k^{(2)0}Y_l^{(2)2}+Y_kY_l^{(3)1}+Y_k^{(3)1}Y_l+Y_k^{(3)3}Y_l^*+Y_k^*Y_l^{(3)3})-k^2E_{jkl}(4Y_k^{(2)0}Y_l^{(2)2}+Y_kY_l^{(3)1}+Y_k^{(3)1}Y_l\\&+Y_k^{(3)3}Y_l^*+9Y_k^*Y_l^{(3)3})-k^2F_{jkl}(Y_kY_l^{(3)1}+Y_k^{(3)1}Y_l-3Y_k^{(3)3}Y_l^*-3Y_k^*Y_l^{(3)3})+ikQ_{jkl}(2Y_k^{(2)0}Y_l^{(2)2}+Y_kY_l^{(3)1}+Y_k^{(3)1}Y_l\\&-Y_k^{(3)3}Y_l^*+3Y_k^*Y_l^{(3)3})+G_{jklm}|_0(Y_k^{(2)0}Y_lY_m+Y_kY_l^{(2)0}Y_m+Y_kY_lY_m^{(2)0}+Y_kY_l^{(2)2}Y_m^*+Y_kY_l^*Y_m^{(2)2}+Y_k^{(2)2}Y_lY_m^*\\&+Y_k^{(2)2}Y_l^*Y_m+Y_k^*Y_l^{(2)2}Y_m+Y_k^*Y_lY_m^{(2)2})-k^2H_{jklm}(Y_k^{(2)0}Y_lY_m+Y_kY_l^{(2)0}Y_m+Y_kY_l^{(2)2}Y_m^*+4Y_kY_l^*Y_m^{(2)2}+Y_k^{(2)2}Y_lY_m^*\\&+Y_k^{(2)2}Y_l^*Y_m+Y_k^*Y_l^{(2)2}Y_m+4Y_k^*Y_lY_m^{(2)2})+k^2L_{jklm}(-Y_k^{(2)0}Y_lY_m+2Y_kY_l^{(2)2}Y_m^*+2Y_kY_l^*Y_m^{(2)2}+Y_k^{(2)2}Y_lY_m^*\\&+Y_k^{(2)2}Y_l^*Y_m-2Y_k^*Y_l^{(2)2}Y_m-2Y_k^*Y_lY_m^{(2)2}),\end{aligned}$$

$$\begin{aligned}\pi_j^{(4)0}=&D_{jkl}|_0[Y_k^{(2)0}Y_l^{(2)0}+Y_k(Y_l^{(3)1})^*+Y_k^{(3)1}Y_l^*+Y_k^*Y_l^{(3)1}+(Y_k^{(3)1})^*Y_l+Y_k^{(2)2}(Y_l^{(2)2})^*+(Y_k^{(2)2})^*Y_l^{(2)2}]+k^2(F_{jkl}-E_{jkl})\\&\times(Y_k(Y_l^{(3)1})^*+Y_k^{(3)1}Y_l^*+Y_k^*Y_l^{(3)1}+(Y_k^{(3)1})^*Y_l+4Y_k^{(2)2}(Y_l^{(2)2})^*+4(Y_k^{(2)2})^*Y_l^{(2)2})-ikQ_{jkl}[Y_k(Y_l^{(3)1})^*+Y_k^{(3)1}Y_l^*\\&-Y_k^*Y_l^{(3)1}-(Y_k^{(3)1})^*Y_l+2Y_k^{(2)2}(Y_l^{(2)2})^*-2(Y_k^{(2)2})^*Y_l^{(2)2}]+G_{jklm}|_0[Y_kY_l^*Y_m^{(2)0}+Y_k^*Y_lY_m^{(2)0}+Y_k^*Y_l^{(2)0}Y_m\end{aligned}$$

$$+Y_kY_l^{(2)0}Y_m^*+Y_k^{(2)0}Y_lY_m^*+Y_k^{(2)0}Y_l^*Y_m+Y_k^{(2)2}Y_l^*Y_m^*+Y_k^*Y_l^{(2)2}Y_m^*+Y_k^*Y_l^*Y_m^{(2)2}+(Y_k^{(2)2})^*Y_lY_m+Y_k(Y_l^{(2)2})^*Y_m$$
$$+Y_kY_l(Y_m^{(2)2})^*]-k^2H_{jklm}[+Y_k^*Y_l^{(2)0}Y_m+Y_kY_l^{(2)0}Y_m^*+Y_k^{(2)2}Y_l^*Y_m^*+Y_k^*Y_l^{(2)2}Y_m^*+4Y_k^*Y_l^*Y_m^{(2)2}+(Y_k^{(2)2})^*Y_lY_m$$
$$+Y_k(Y_l^{(2)2})^*Y_m+4Y_kY_l(Y_m^{(2)2})^*+Y_k^{(2)0}Y_lY_m^*+Y_k^{(2)0}Y_l^*Y_m]+k^2L_{jklm}[2Y_k^*Y_l^{(2)2}Y_m^*+2Y_k^*Y_l^*Y_m^{(2)2}-Y_k^{(2)2}Y_l^*Y_m^*$$
$$-(Y_k^{(2)2})^*Y_lY_m+2Y_k(Y_l^{(2)2})^*Y_m+2Y_kY_l(Y_m^{(2)2})^*+Y_k^{(2)0}Y_lY_m^*+Y_k^{(2)0}Y_l^*Y_m],$$

$$\pi_j^{(4)1}=D_{jkl}|_0\left(Y_kY_l^{(3)0}+Y_k^{(3)0}Y_l+i\frac{\partial Y_k^*}{\partial k}Y_l^{(2)2}+iY_k^{(2)2}\frac{\partial Y_l^*}{\partial k}\right)-k^2E_{jkl}\left(Y_k^{(3)0}Y_l+4i\frac{\partial Y_k^*}{\partial k}Y_l^{(2)2}+iY_k^{(2)2}\frac{\partial Y_l^*}{\partial k}\right)-2ikE_{jkl}Y_k^{(2)2}Y_l^*$$
$$+Q_{jkl}(Y_kY_l^{(2)0}+Y_k^{(2)2}Y_l^*)+kQ_{jkl}\left(Y_k^{(2)2}\frac{\partial Y_l^*}{\partial k}-2\frac{\partial Y_k^*}{\partial k}Y_l^{(2)2}+iY_k^{(3)0}Y_l\right)+2k^2F_{jkl}\left(i\frac{\partial Y_k^*}{\partial k}Y_l^{(2)2}+iY_k^{(2)2}\frac{\partial Y_l^*}{\partial k}\right)$$
$$+ikF_{jkl}(Y_kY_l^{(2)0}+Y_k^{(2)0}Y_l+2Y_k^{(2)2}Y_l^*+2Y_k^*Y_l^{(2)2})+i(G_{jklm}|_0-k^2H_{jklm})\left(Y_k\frac{\partial Y_l^*}{\partial k}Y_m+Y_kY_l\frac{\partial Y_m^*}{\partial k}+\frac{\partial Y_k^*}{\partial k}Y_lY_m\right)$$
$$+ik^2L_{jklm}\left(Y_k\frac{\partial Y_l^*}{\partial k}Y_m+Y_kY_l\frac{\partial Y_m^*}{\partial k}-\frac{\partial Y_k^*}{\partial k}Y_lY_m\right)+ikL_{jklm}(Y_kY_l^*Y_m+Y_kY_lY_m^*)-2ikH_{jklm}Y_kY_lY_m^*.$$

Note that a partial derivative with respect to k means the derivative at the critical value $k=k_c$. The last inhomogeneity is given by

$$\pi_j^{(5)1}=D_{jkl}|_0[Y_kY_l^{(4)0}+Y_k^{(4)0}Y_l+Y_k^{(3)1}Y_l^{(2)0}+Y_k^{(2)0}Y_l^{(3)1}+Y_k^{(4)2}Y_l^*+Y_k^*Y_l^{(4)2}+Y_k^{(2)2}(Y_l^{(3)1})^*+(Y_k^{(3)1})^*Y_l^{(2)2}+Y_k^{(3)3}(Y_l^{(2)2})^*$$
$$+(Y_k^{(2)2})^*Y_l^{(3)3}]-k^2E_{jkl}[Y_k^{(4)0}Y_l+Y_k^{(2)0}Y_l^{(3)1}+Y_k^{(4)2}Y_l^*+4Y_k^*Y_l^{(4)2}+Y_k^{(2)2}(Y_l^{(3)1})^*+4(Y_k^{(3)1})^*Y_l^{(2)2}$$
$$+4Y_k^{(3)3}(Y_l^{(2)2})^*+9(Y_k^{(2)2})^*Y_l^{(3)3}]+2k^2F_{jkl}[Y_k^{(4)2}Y_l^*+Y_k^*Y_l^{(4)2}+Y_k^{(2)2}(Y_l^{(3)1})^*+(Y_k^{(3)1})^*Y_l^{(2)2}+3Y_k^{(3)3}(Y_l^{(2)2})^*$$
$$+3(Y_k^{(2)2})^*Y_l^{(3)3}]+ikQ_{jkl}[Y_k^{(4)0}Y_l+Y_k^{(2)0}Y_l^{(3)1}-Y_k^{(4)2}Y_l^*-Y_k^{(2)2}(Y_l^{(3)1})^*+2Y_k^*Y_l^{(4)2}+2(Y_k^{(3)1})^*Y_l^{(2)2}$$
$$-2Y_k^{(3)3}(Y_l^{(2)2})^*+3(Y_k^{(2)2})^*Y_l^{(3)3}]+G_{jklm}|_0[(Y_k^{(2)2})^*Y_lY_m^{(2)2}+(Y_k^{(2)2})^*Y_l^{(2)2}Y_m+Y_k^*Y_l^{(2)2}Y_m^{(2)0}+Y_k^{(2)2}Y_l^*Y_m^{(2)0}$$
$$+Y_k^*Y_l^{(2)0}Y_m^{(2)2}+Y_k^{(2)2}Y_l^{(2)0}Y_m^*+Y_k^{(2)2}(Y_l^{(2)2})^*Y_m+Y_k^{(2)2}Y_l(Y_m^{(2)2})^*+Y_kY_l^{(2)2}(Y_m^{(2)2})^*+Y_k(Y_l^{(2)2})^*Y_m^{(2)2}$$
$$+Y_kY_l^{(2)0}Y_m^{(2)0}+Y_k^{(2)0}Y_lY_m^{(2)0}+Y_k^{(2)0}Y_l^{(2)0}Y_m+Y_k^{(2)0}Y_l^{(2)2}Y_m^*+Y_k^{(2)0}Y_l^*Y_m^{(2)2}+Y_k^*Y_l^*Y_m^{(3)3}+Y_k^{(3)3}Y_l^*Y_m^*+Y_k^*Y_l^{(3)3}Y_m^*$$
$$+(Y_k^{(3)1})^*Y_lY_m+Y_k^*Y_l^{(3)1}Y_m+Y_k^*Y_lY_m^{(3)1}+Y_k^{(3)1}Y_lY_m^*+Y_kY_l^{(3)1}Y_m^*+Y_kY_l(Y_m^{(3)1})^*+Y_k^{(3)1}Y_l^*Y_m+Y_k(Y_l^{(3)1})^*Y_m$$
$$+Y_kY_l^*Y_m^{(3)1}]-k^2H_{jklm}[4(Y_k^{(2)2})^*Y_lY_m^{(2)2}+(Y_k^{(2)2})^*Y_l^{(2)2}Y_m+4Y_k^*Y_l^{(2)0}Y_m^{(2)2}+Y_k^{(2)2}Y_l^{(2)0}Y_m^*+Y_k^{(2)2}(Y_l^{(2)2})^*Y_m$$
$$+4Y_k^{(2)2}Y_l(Y_m^{(2)2})^*+4Y_kY_l^{(2)2}(Y_m^{(2)2})^*+4Y_k(Y_l^{(2)2})^*Y_m^{(2)2}+Y_k^{(2)0}Y_l^{(2)0}Y_m+Y_k^{(2)0}Y_l^{(2)2}Y_m^*+4Y_k^{(2)0}Y_l^*Y_m^{(2)2}$$
$$+9Y_k^*Y_l^*Y_m^{(3)3}+Y_k^{(3)3}Y_l^*Y_m^*+Y_k^*Y_l^{(3)3}Y_m^*+(Y_k^{(3)1})^*Y_lY_m+Y_k^*Y_l^{(3)1}Y_m+Y_k^*Y_lY_m^{(3)1}+Y_k^{(3)1}Y_lY_m^*+Y_kY_l^{(3)1}Y_m^*$$
$$+Y_kY_l(Y_m^{(3)1})^*+Y_k^{(3)1}Y_l^*Y_m+Y_k(Y_l^{(3)1})^*Y_m+Y_kY_l^*Y_m^{(3)1}]+k^2L_{jklm}[2Y_k^{(2)2}(Y_l^{(2)2})^*Y_m-2(Y_k^{(2)2})^*Y_lY_m^{(2)2}$$
$$+2Y_k^{(2)2}Y_l(Y_m^{(2)2})^*-2(Y_k^{(2)2})^*Y_l^{(2)2}Y_m+4Y_kY_l^{(2)2}(Y_m^{(2)2})^*+4Y_k(Y_l^{(2)2})^*Y_m^{(2)2}+2Y_k^{(2)0}Y_l^{(2)2}Y_m^*+2Y_k^{(2)0}Y_l^*Y_m^{(2)2}$$
$$+3Y_k^*Y_l^*Y_m^{(3)3}-Y_k^{(3)3}Y_l^*Y_m^*+3Y_k^*Y_l^{(3)3}Y_m^*-(Y_k^{(3)1})^*Y_lY_m-Y_k^*Y_l^{(3)1}Y_m-Y_k^*Y_lY_m^{(3)1}+Y_k^{(3)1}Y_lY_m^*+Y_kY_l^{(3)1}Y_m^*$$
$$+Y_kY_l(Y_m^{(3)1})^*+Y_k^{(3)1}Y_l^*Y_m+Y_k(Y_l^{(3)1})^*Y_m+Y_kY_l^*Y_m^{(3)1}].$$

Finally we give the coefficients of the quadratic equation (4.6)

$$a_1=2b_rq^2-2R^2\left(c_r+2R^2d_r+(k-k_c)\frac{\partial c_r}{\partial k}\bigg|_0\right),$$

$$b_1=-2q\left(u-2b_i(k-k_c)+2R^2\frac{\partial c_i}{\partial k}\bigg|_0+R^2a_r\right),$$

$$a_0 = -q^2 b_r \left(-b_r q^2 + 2R^2 \left[c_r + 2R^2 d_r + (k-k_c) \frac{\partial c_r}{\partial k}\bigg|_0 \right] \right) - q^2 b_i \left(-b_i q^2 + 2R^2 \left[c_i + 2R^2 d_i + (k-k_c) \frac{\partial c_i}{\partial k}\bigg|_0 \right] \right)$$
$$- q^2 \left(2b_r (k-k_c) - R^2 \frac{\partial c_r}{\partial k}\bigg|_0 \right) \left(2b_r (k-k_c) - 3R^2 \frac{\partial c_r}{\partial k}\bigg|_0 + 2R^2 a_i \right)$$
$$- q^2 \left(u - 2b_i (k-k_c) + R^2 \frac{\partial c_i}{\partial k}\bigg|_0 \right) \left(u - 2b_i (k-k_c) + 3R^2 \frac{\partial c_i}{\partial k}\bigg|_0 + 2R^2 a_r \right),$$

$$b_0 = q^3 b_i \left(2b_r (k-k_c) - 3R^2 \frac{\partial c_r}{\partial k}\bigg|_0 + 2R^2 a_i \right) - q^3 b_r \left(u - 2b_i (k-k_c) + 3R^2 \frac{\partial c_i}{\partial k}\bigg|_0 + 2R^2 a_r \right)$$
$$+ q \left(2b_r (k-k_c) - R^2 \frac{\partial c_r}{\partial k}\bigg|_0 \right) \left(-q^2 b_i + 2R^2 \left[c_i + 2R^2 d_i + (k-k_c) \frac{\partial c_i}{\partial k}\bigg|_0 \right] \right)$$
$$+ q \left(u - 2b_i (k-k_c) + R^2 \frac{\partial c_i}{\partial k}\bigg|_0 \right) \left(-q^2 b_r + 2R^2 \left[c_r + 2R^2 d_r + (k-k_c) \frac{\partial c_r}{\partial k}\bigg|_0 \right] \right),$$

where the phase velocity u [cf. (4.1)] can be calculated by means of

$$u = b_i (k-k_c) - \frac{\partial c_i}{\partial k}\bigg|_0 R^2 - R^2 (c_i + d_i R^2)/(k-k_c).$$

[1] M.C. Cross and P.C. Hohenberg, Rev. Mod. Phys. **65**, 851 (1993).

[2] K. Ohe and M. Hashimoto, J. Appl. Phys. **58**, 2975 (1985).

[3] C. Wilke, R.W. Leven, and H. Deutsch, Phys. Lett. A **136**, 114 (1989).

[4] Ji-Bin Du, Chi-Hui Chiang, and Lin I, Phys. Rev. E **54**, 1829 (1996).

[5] R.N. Franklin, *Plasma Phenomena in Gas Discharges* (Clarendon Press, Oxford, 1976).

[6] P.S. Landa, *Self-Oscillations in Distributed Systems* (Nauka, Novosibirsk, Russia, 1983).

[7] B.P. Koch, N. Goepp, and B. Bruhn, Phys. Rev. E **56**, 2118 (1997). In this paper and in [8] there are two misprints in the collision rates. The corresponding correct expressions are $z_{0m} = 5.294 \times 10^{-13} (E/p_0)^{2.015}$ cm^3 s^{-1}, $p_w = 4{,}362 \times 10^2 (E/p_0)^{8.932}$V cm^{3}s^{-1}.

[8] B. Bruhn, B.P. Koch, and N. Goepp, Physica D **115**, 353 (1998).

[9] N. Bekki, J. Phys. Soc. Jpn. **50**, 659 (1981).

[10] H. van Saarloos and P.C. Hohenberg, Physica D **56**, 303 (1992).

[11] H. Chaté, in *Spatio-Temporal Patterns in Nonequilibrium Complex Systems*, edited by P.E. Cladis and P. Palffy-Muhoray (Addison-Wesley, Reading, MA, 1995), p. 33.

[12] B. Bruhn, B.P. Koch, and P. Jonas, Phys. Rev. E **58**, 3793 (1998).

[13] H. Achterberg and J. Michel, Ann. Phys. (Leipzig) **2**, 365 (1959).

[14] A. Dinklage, B. Bruhn, H. Deutsch, P. Jonas, B.-P. Koch, and C. Wilke, Phys. Plasmas **5**, 833 (1998).

[15] W. Eckhaus and G. Iooss, Physica D **39**, 124 (1989).

[16] R.J. Deissler and H.R. Brand, Phys. Rev. Lett. **81**, 3856 (1998).

[17] A. Doelman and W. Eckhaus, Physica D **53**, 249 (1991).

[18] A.C. Newell, in *Lectures in Applied Mathematics* (American Mathematical Society, Providence, RI, 1974), Vol. 15, p. 157.

[19] P. Manneville, *Dissipative Structures and Weak Turbulence* (Academic Press, New York, 1990), p. 325.

[20] J. Duan, in *Fields Institute Communications* (American Mathematical Society, Providence, RI, 1996), Vol. 5, p. 165.

[21] P. Jonas, B. Bruhn, B.P. Koch, and A. Dinklage, Phys. Plasmas **7**, 729 (2000).

[22] J.T. Stuart and R.C. Diprima, Proc. R. Soc. London, Ser. A **362**, 27 (1978).

[23] A.S. Mikhailov and A.Y. Loskutov, *Foundations of Synergetics II. Complex Patterns* (Springer, Berlin, 1991).

[24] S. Pfau, A. Rutscher, and K. Wojaczek, Beitr. Plasmaphys. **9**, 333 (1969).

[25] A. Garscadden, in *Gaseous Electronics*, edited by M.N. Hirsch and H.J. Oskam (Academic Press, New York, 1978), Vol. I.

[26] B. Janiaud, A. Pumir, D. Bensimon, V. Croquette, H. Richter, and L. Kramer, Physica D **55**, 269 (1992).

[27] N. Mukolobwiez, A. Chiffaudel, and F. Daviaud, Phys. Rev. Lett. **80**, 4661 (1998).